Electronic Raman scattering in thin bismuth films

1991 J. Phys.: Condens. Matter 3 4677

(http://iopscience.iop.org/0953-8984/3/25/014)

J. Phys.: Condens. Matter 3 (1991) 4677–4686. Printed in the UK

Electronic Raman scattering in thin bismuth films

A T Gadzhiev, F M Gashimzade and N B Mustafaev
Institute of Physics, Academy of Sciences of the Azerbaijan SSR, Narimanov Prospekti 33, Baku 370143, USSR

Received 23 July 1990

Abstract. The theory of the electron Raman scattering (ERS) in a size-quantized film within the framework of the Abrikosov–Cohen model for the energy spectrum of Bi is developed. The wavefunctions and spectrum of electrons in the film are obtained. It is shown that the zero boundary conditions must be imposed on the total wavefunction instead of on the envelope. The boundary conditions for the envelope have a complicated form and are similar to those found by Volkov and Pinsker. It is shown that unlike the standard model of the energy spectrum of carriers the scheme of an intraband ERS process with an intermediate state in the valence band is realized within the framework of the Abrikosov–Cohen spectrum. On the basis of the scheme described, the frequency dependence of the ERS differential cross section is calculated. The cross section has a non-zero value for any Δn (Δn is the change in the electron quantum number due to the ERS process) at arbitrary orientation of the polarization vectors of incident and scattered radiation with respect to the film surface.

1. Introduction

Investigation of the electron Raman scattering (ERS) in quasi-two-dimensional systems at present is of great interest. The ERS in semiconducting InSb and PbTe films [1, 2] as well as in $GaAs/Al_xGa_{1-x}As$ heterostructures [3] have been studied previously. Thin Bi films have been shown to be the best material for the ERS realization on the size quantization levels. Owing to the small values of the electron effective mass and the Fermi energy E_F and the large value of mean free path and other physical properties the quantum size effects were for the first time found in thin Bi films [4]. The electronic spectrum of Bi is characterized by large anisotropy and non-parabolicity. There are several models to describe the complicated energy spectrum of Bi. The Abrikosov–Cohen [5, 6] model is adequate for the real spectrum of Bi and at the same time it is convenient for theoretical calculations. The aim of the present paper is to develop the theory of ERS in thin Bi films within the framework of the Abrikosov–Cohen model.

This paper consists of four parts. In section 2 the wavefunctions and spectrum of electrons in a size-quantized Bi film are obtained. It is shown that the zero boundary conditions on the film surfaces for the envelopes of the wavefunction are not correct in general. In the case of the many-band model such boundary conditions lead to envelopes not satisfying the initial equations. It is necessary to impose zero boundary conditions on the total wavefunction instead.

In section 3 the possible schemes of the ERS process in the Bi film are considered. It

0953-8984/91/254677 + 10 $03.50

is shown that the ERS process takes place at arbitrary orientation of the polarization vectors of the incident and scattered radiations with respect to the film surface.

In section 4 the scheme in which the initial n and final n' states of electronic system are in the conduction band but the intermediate state n'' is in the valence band is studied in more detail. If $n \neq n'$, this scheme is forbidden for the standard model of the energy spectrum of carriers. On the basis of the scheme described, the frequency dependence of the ERS differential cross section (DCS) is calculated.

The results of the present paper can be useful for analysis of the ERS experiments in thin Bi films.

2. The electron wavefunctions and spectrum in a thin Bi film

The electron wavefunctions and spectrum were derived from the stationary Schrödinger equation

$$\{\hat{H} + U(r)\}\psi(r) = E\psi(r) \tag{2.1}$$

where $\hat{H}$ is the free Hamiltonian and $U(r)$ is a potential which localizes a particle in the film. If $U(r)$ changes slightly within the elementary cell, the solution of equation (2.1) can be tried in a form [7]

$$\psi(r) = \sum_j F_j(r)\varphi_j(r) \tag{2.2}$$

where $\varphi_j(r)$ is the Bloch function corresponding to the jth band extremum and $F_j(r)$ is the envelope function. If $U(r) = 0$, the envelope has the form

$$F_j(r) = C_j(k)\exp(ik \cdot r). \tag{2.3}$$

The Fermi surface of electrons in Bi consists of three valleys which are tilted at the angle $\theta = 6°\,23'$ with respect to the basal plane. These valleys transfer into each other under a rotation of $\pm 120°$ around the trigonal axis z. We considered the case when the film plane is normal to z. We also neglected the small tilt angle θ.

It was assumed that, within the film, $U(r)$ is a constant (is equal to zero) but, at the surfaces of film, $U(r) \to \infty$. Within the framework of such an assumption the effective-mass approximation is valid. A periodicity in the film plane (the x–y plane) remains. Therefore the solution of the Schrödinger equation can be attempted in the form of plane waves, but along the z axis the periodicity is broken. In this direction the solution must be attempted in a general form. A concrete form of the solution is governed by the boundary conditions on the film surface.

By analogy with (2.3) we choose the envelope in a form

$$F_j(r) = f_j(z)\exp(ik_\perp \cdot \rho). \tag{2.4}$$

Here $k_\perp$ and ρ are the wavevector and position vector in the film plane and $f_j(z)$ are the unknown functions. The solution of equation (2.1) was obtained using the effective Hamiltonian of the Abrikosov–Cohen model:

$$\mathcal{H} = \begin{pmatrix} \hat{K}_0 - E_g & 0 & t \cdot \hat{p} & u \cdot \hat{p} \\ 0 & \hat{K}_0 - E_g & -(u^* \cdot \hat{p}) & t^* \cdot \hat{p} \\ t^* \cdot \hat{p} & -(u \cdot \hat{p}) & \hat{K}_1 & 0 \\ u^* \cdot \hat{p} & t \cdot \hat{p} & 0 & \hat{K}_1 \end{pmatrix}. \tag{2.5}$$

Here E_g is an energy gap at the L point of the Brillouin zone; $\hat{K}_0$ describes the interaction between the valence band and the other bands with the exception of the conduction band; $\hat{K}_1$ describes the interaction between the conduction band and the other bands with the exception of the valence band; t and u are the matrix elements of velocity. In the Abrikosov–Cohen model the dependence of energy upon the wavevector component along the y axis (the direction of the isoenergetic surface elongation) is determined by $\hat{K}_0$ and $\hat{K}_1$ mainly. Such an assumption allows one to explain the large difference between the values of the electron effective-mass components in Bi: $m_{x,z} \simeq 10^{-2} m_0$ and $m_y \simeq m_0$ (m_0 is the mass of a free electron).

We choose the wavefunction (for one valley) in the column form

$$\psi(\boldsymbol{r}) = \begin{pmatrix} f_1(z) \\ f_2(z) \\ f_3(z) \\ f_4(z) \end{pmatrix} \exp(i\boldsymbol{k}_\perp \cdot \boldsymbol{\rho}) \tag{2.6}$$

which is the equivalent of (2.2) for the case $j = \overline{1,4}$ if (2.4) is taken into account.

Using equations (2.5) and (2.6) a set of four linear homogeneous differential equations can be obtained from (2.1). The substitution of these differential equations into each other leads to

$$\kappa^2 f_j(z) + \nabla_z^2 f_j(z) = 0 \tag{2.7}$$

where

$$\kappa^2 = [(K_0 - E_g - E)(K_1 - E) - (\hbar k_x V_x)^2]/(\hbar V_z)^2. \tag{2.8}$$

In (2.8) the following notation is used: $K_0 = -(\hbar k_y)^2/2m_y'$; $K_1 = (\hbar k_y)^2/2m_y$; $V_\alpha^2 = u_\alpha^* u_\alpha + t_\alpha^* t_\alpha$.

A general solution of equation (2.7) is

$$f_j(z) = A_j \cos(\kappa z) + B_j \sin(\kappa z). \tag{2.9}$$

The coefficients A_j and B_j and the eigenvalues of κ are determined from the boundary conditions. If the film potential is approximated by a square well with infinite walls, it is assumed usually that the envelopes (2.9) vanish at the surfaces of the film, that is

$$f_j(z_0) = 0 \tag{2.10}$$

where z_0 has two values: $z_0 = 0$ and $z_0 = d$ (d is the film thickness). The envelopes satisfying (2.10) are the partial solutions of equation (2.7) and have the form

$$f_j(z) = B_j \sin(\pi n z/d) \qquad n = 1, 2, 3, \ldots. \tag{2.11}$$

In the case of the parabolic band model the total wavefunction also vanishes at the film surfaces under condition (2.10). However, if the non-parabolicity of the wavefunction is taken into account, the condition (2.10) does not coincide with the condition

$$\psi(\boldsymbol{\rho}, z_0) = 0. \tag{2.12}$$

It may be shown that our initial set of differential equations is not satisfied by (2.11). This is because it is impossible to construct all $f_j(z)$ simultaneously in the form of partial solutions. The functions $f_j(z)$ are related to each other via the initial set of equations.

Thus a conclusion can be made that it is necessary to impose zero boundary conditions

on the total wavefunction. It may be shown that (2.12) leads to the following boundary condition for the envelopes:

$$[1 + R_j(z_0)\nabla_z]f_j(z_0) = 0. \tag{2.13}$$

Condition (2.13) coincides formally with those obtained in [8]. In [8], R is a constant which yields information about the surface properties of the crystal. In our case there is a relation between $R_j(z_0)$ and the values of the Bloch functions fixed on the film surfaces. So $R_j(z_0)$ in (2.13) can be treated as the characteristics of the film surface in terms of such a relation.

Substituting equation (2.9) into equation (2.13) we derive a set of two equations (one of these equations is algebraic but the other is transcendental). This set has a solution if the following condition is valid:

$$\tan(\kappa d) = \{[R_j(0) - R_j(d)]/[1 + \kappa^2 R_j(0)R_j(d)]\}\kappa. \tag{2.14}$$

Let us assume that the number of elementary cells along the film thickness is an integer, i.e. $d = Na_0$ (N is an integer and a_0 is a lattice constant). Taking into account the periodicity of the Bloch functions, we may show that $R_j(0) = R_j(d)$. By virtue of this equality equation (2.14) takes the quasi-classical form

$$\kappa = \pi n/d \qquad n = 1, 2, 3, \ldots. \tag{2.15}$$

It follows from (2.8) and (2.15) that the electron spectrum in a thin Bi film has the form

$$(K_0 - E_g - E)(K_1 - E) = (\hbar k_x V_x)^2 + (\hbar\pi V_z n/d)^2. \tag{2.16}$$

It may be shown that the conduction and valence bands in a thin Bi film are described by the following wavefunctions:

$$|\nu\sigma n\rangle = \Gamma_{\nu\sigma n} G_{\nu n} \exp(ik_\perp \cdot \rho)[A_{\nu\sigma n} \cos(\pi n z/d) + i(\hbar\pi n/d)B_{\nu\sigma n} \sin(\pi n z/d)]. \tag{2.17}$$

Here $\nu \equiv c, v$ is the band index and $\sigma = 1, 2$ is the spin index. The other notation has a cumbersome form and is given in the appendix.

3. The ERS processes in thin Bi film

Calculating the ERS DCS we made use of the definition of the DCS from [9]. The expression for the DCS in a size-quantized film is as follows:

$$\frac{d^2\Pi}{d\Omega\, d\omega} = \frac{\hbar(e^2/m_0c^2)^2}{\omega_0/\omega_1} \sum_{\substack{n'n \\ \sigma'\sigma}} |S^{e_1,e_0}_{n'\sigma',n\sigma}|^2\, \delta(E_{k_\perp n'} - E_{k_\perp n} - \hbar\omega) \tag{3.1}$$

where

$$S^{e_1,e_0}_{n'\sigma',n\sigma} = \frac{1}{m_0} \sum_{k_\perp n''\sigma''} \left(\frac{\langle n'\sigma'|e_1 \cdot p|n''\sigma''\rangle\langle n''\sigma''|e_0 \cdot p|n\sigma\rangle}{E_{k_\perp n} - E_{k_\perp n''} + \hbar\omega_0} + \frac{\langle n'\sigma'|e_0 \cdot p|n''\sigma''\rangle\langle n''\sigma''|e_1 \cdot p|n\sigma\rangle}{E_{k_\perp n} - E_{k_\perp n''} - \hbar\omega_1} \right). \tag{3.2}$$

Here (e_0, ω_0) and (e_1, ω_1) are the polarization vectors and frequencies of the incident and scattered radiation, respectively; $\omega = \omega_0 - \omega_1$ is a frequency shift; (n, σ), (n', σ') and (n'', σ'') are the quantum and spin numbers of the initial, final and intermediate states, respectively. The other notation has the usual meanings.

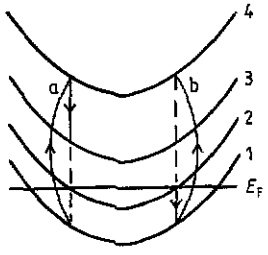

Figure 1. Illustration of the intraband ERS process with the intermediate state in the conduction band.

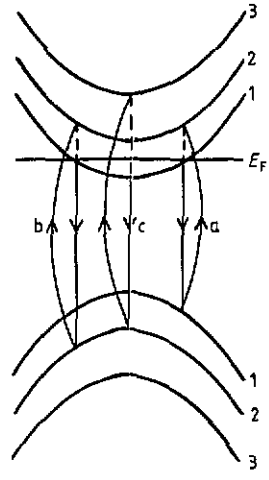

Figure 2. Illustration of the intraband ERS process with the intermediate state in the valence band.

We established from calculations of (3.2) on the basis of the wavefunctions (2.17) that the processes of ERS given in sections 3.1–3.4 are possible.

3.1. The intraband ERS process with the intermediate state in the conduction band

Figure 1 illustrates this process in the situation when two subbands are filled. There are two process schemes. According to the first scheme (scheme a), only one electron takes part in the process. According to the second scheme (scheme b), two electrons take part in the process. If we restrict ourselves only to optical transitions between four subbands, the process occurs in the following way.

In scheme a, the electron absorbs the photon with frequency ω_0 and is lifted from the $n = 1$ subband up to the $n = 4$ subband (if the subbands have numbers n of the same parity, the matrix elements of the intraband optical transitions are equal to zero [10]). Then the electron emits a photon with frequency ω_1 and drops to the $n = 3$ subband. The scheme described corresponds to a real direct transition from the initial state $n = 1$ to a final state $n' = 3$.

In scheme b, the electron from the $n = 1$ subband absorbs a photon and is lifted to the $n = 4$ subband. Then the other electron from the $n = 2$ subband emits a photon and immediately occupies a vacant state in the $n = 1$ subband. The scheme described corresponds to a real transition from the initial state $n = 2$ to a final state $n' = 4$.

As one can see from both schemes, the values of $\Delta n = n' - n$ are even. We must note that the process takes place at the arbitrary orientation of e_0 and e_1 with respect to the film surface. This is the main difference from the results of [1].

3.2. The intraband ERS process with the intermediate state in the valence band

Figure 2 illustrates this process in the situation when one subband is filled. Here we restrict ourselves for simplicity to the transitions between six subbands (three subbands of the valence band and three subbands of the conduction band). We must note that only matrix elements of the interband optical transitions with $n_v = n_c$ and $n_v + n_c = 2N + 1$ (N is integer) are not equal to zero. Therefore three process schemes are possible.

In scheme a, the electron from the state $n_v = 1$ in the valence band is lifted to the state $n_c = 2$ in the conduction band. Then the other electron from the state $n_c = 1$ in the conduction band drops and occupies the vacant state $n_v = 1$ in the valence band. The scheme described corresponds to a real transition from the initial state $n_c = 1$ to the final state $n_c' = 2$.

In scheme b, the first electron is lifted from the state $n_v = 2$ up to the state $n_c = 2$. Then the second electron drops from the state $n_c = 1$ to the vacant state $n_v = 2$. The scheme described also corresponds to the real transition from the initial state $n_c = 1$ to the final state $n_c' = 2$.

In scheme c, the electron from the state $n_v = 2$ is lifted up to the state $n_c = 3$. The other electron from the state $n_c = 1$ falls to the vacant state $n_v = 2$. The scheme described corresponds to a real transition from the initial state $n_c = 1$ to the final state $n_c' = 3$.

The difference $\Delta n_c = n_c' - n_c$ is odd according to the first scheme a and the second scheme b and is even according to the third scheme c. In all schemes the transitions occur at arbitrary orientation of e_0 and e_1 with respect to the film surface.

We must note that the intraband ERS process with the intermediate state in the valence band is not realized within the framework of the standard model for the energy spectrum of carriers. This is associated with the fact that only interband optical transitions with the selection rule $n_v = n_c$ are allowed in the standard model.

3.3. The interband ERS process with the intermediate state in the conduction band

Figure 3 illustrates this process in the situation when one subband is filled. If we restrict ourselves to the transitions between four subbands (two subbands of the valence band and two subbands of the conduction band), the process occurs in the following ways.

In scheme a, the electron from the state $n_v = 2$ in the valence band is lifted to the state $n_c = 2$ in the conduction band and then falls to the vacant state in the $n_c = 1$ subband. The scheme described corresponds to a real transition from the initial state $n_v = 2$ to the final state $n_c' = 1$.

In scheme b, the electron from the state $n_v = 1$ is lifted to the state $n_c = 2$ and then falls to the vacant state in the subband $n_c = 1$. The scheme described corresponds to a real transition from the initial state $n_v = 1$ to the final state $n_c' = 1$.

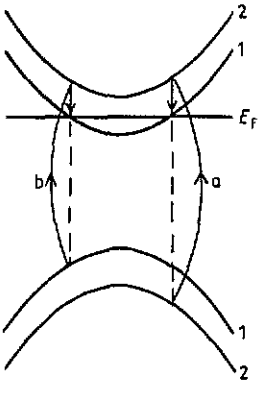

Figure 3. Illustration of the interband ERS process with the intermediate state in the conduction band.

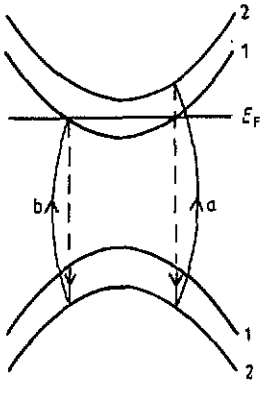

Figure 4. Illustration of the interband ERS process with the intermediate state in the valence band.

3.4. The interband ERS process with the intermediate state in the valence band

Two electrons take part in the process (figure 4). Two schemes are possible.

In scheme a, the first electron from the state $n_v = 2$ is lifted to the state $n_c = 2$. The second electron from the state $n_v = 1$ falls to the vacant state in the $n_v = 2$ subband. The scheme described corresponds to the real transition from the initial state $n_v = 1$ to the final state $n_c' = 2$.

In scheme b, the electron from the state $n_v = 2$ is lifted to the vacant state in the $n_c = 1$ subband. The other electron from $n_v = 1$ occupies the vacant state in the $n_v = 2$ subband. The scheme described corresponds to a real transition from the initial state $n_v = 1$ to the final state $n_c' = 1$.

As mentioned above, only the interband optical transitions with the selection rule $n_v = n_c$ are allowed in the framework of the standard model of spectrum. Therefore both schemes b of the interband ERS process (with the intermediate state in the conduction band and with the intermediate state in the valence band) is not realized in the standard model. Another difference between our results and the results of [2, 3] is that within the framework of the Abrikosov–Cohen model the interband ERS processes take place at arbitrary orientation of e_0 and e_1 with respect to the film surface.

4. DCS of the intraband ERS with the intermediate state in valence band

In this section the ERS process with the intermediate state in the valence band is studied in detail. Physically such a process has a high probability. However, as was mentioned above, this process is not realized within the framework of the standard model of the spectrum. In the case of the Abrikosov–Cohen model the process considered takes place at arbitrary orientation of the polarization vectors of incident e_0 and scattered e_1 radiations with respect to the film surface. The conventional geometry of the ERS experiments is $e_0 \| e_1 \perp z$. Therefore only the results of calculation for such a geometry are reported in the present paper. Calculations were made on the basis of (3.1) and (2.17). The parameters of the Abrikosov–Cohen model were taken from [11] (at the liquid-helium temperature, $E_g = 13.6$ meV, $V_x = 0.91 \times 10^8$ cm s^{-1}, $m_y = 1.2m_0$, $V_z = 0.56 \times 10^8$ cm s^{-1} and $m_y/m_y' = 2$).

The graphs of the frequency dependence of the DCS have the least complicated form in Bi films with $d < 80$ nm. This is because in such films, at the liquid-helium temperature, only one subband is filled (the thickness dependence of the Fermi energy E_F was calculated within the framework of the Abrikosov–Cohen model in [12]). Therefore, only $n_c = 1$ can be an initial state of the electron system in the ERS process. The results of calculation of the frequency dependence of DCS in a Bi film 70 nm thick at $T = 4.2$ K are given in figures 5–7. As one can see in these figures, the ERS spectrum consists of a number of lines which do not overlap each other. The width of spectral line is governed by the condition

$$E_{k_\perp n_c} \leqslant E_F < E_{k_\perp n_c'}. \tag{4.1}$$

The first spectral line (1.47×10^{13} s$^{-1} < \omega < 2.40 \times 10^{13}$ s^{-1}) corresponds to transitions from the initial state $n_c = 1$ to the final state $n_c' = 2$. The second spectral line (3.39×10^{13} s$^{-1} < \omega < 4.88 \times 10^{13}$ s^{-1}) corresponds to the transitions between the states

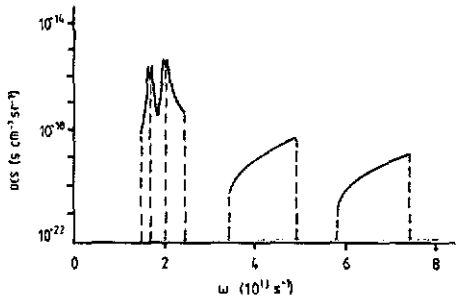

Figure 5. Plot of the ERS DCS as a function of the frequency shift ω at a temperature of 4.2 K for the case when a Bi film 70 nm thick is illuminated with radiation of wavelength 16.3 μm.

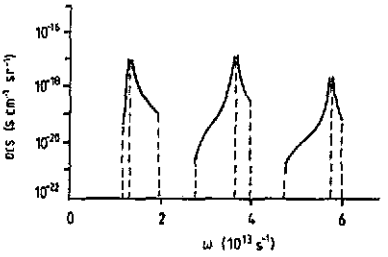

Figure 6. Plot of the ERS DCS as a function of the frequency shift ω at a temperature of 4.2 K for the case when a Bi film 70 nm thick is illuminated with radiation of wavelength 14.0 μm.

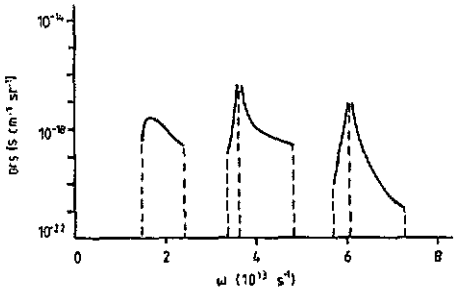

Figure 7. Plot of the ERS DCS as a function of the frequency shift ω at a temperature of 4.2 K for the case when a Bi film 70 nm thick is illuminated with radiation of wavelength 12.1 μm.

$n_c = 1$ and $n_c' = 3$. The third spectral line ($5.80 \times 10^{13}\ s^{-1} < \omega < 7.37 \times 10^{13}\ s^{-1}$) corresponds to transitions between $n_c = 1$ and $n_c' = 4$.

Plots of the frequency dependence of DCS in films with $d > 80$ nm are not given in the present paper. We note that in these films the ERS spectra have a rather complicated form. Thus the ERS spectrum of a Bi film 100 nm thick at $T = 4.2$ K (two subbands are filled) in the frequency region $\omega < 1.86 \times 10^{13}\ s^{-1}$ consists of two lines with $\Delta n_c = 1$: the first line ($0.77 \times 10^{13}\ s^{-1} < \omega < 1.30 \times 10^{13}\ s^{-1}$) corresponds to the transitions from the initial state $n_c = 1$ to the final state $n_c' = 2$ and the second line ($1.34 \times 10^{13}\ s^{-1} < \omega < 1.72 \times 10^{13}\ s^{-1}$) corresponds to the transitions between the initial $n_c = 2$ and final $n_c' = 3$ states. In the frequency region $\omega > 1.86 \times 10^{13}\ s^{-1}$, spectral lines with $\Delta n_c > 1$ overlap and create a continuous spectral band.

The resonances appear (or disappear) in the ERS spectra with a variation in frequency of the incident radiation. A resonance appears when the distance between the initial and intermediate states is equal to the energy of the scattered photon (the denominator of (3.2) goes to zero). In the case when $\Delta n_c = 2N$ the number of intermediate states is not restricted. The resonance condition has the form

$$\hbar\omega_0/E_g = \gamma + [\gamma^2 + (\pi\hbar V_z/E_g d)^2(n_v''^2 - n_c'^2)]^{1/2} \tag{4.2}$$

where

$$\gamma = (\hbar\omega/2E_g)[1 + (\pi V_z/\omega d)^2(n_c'^2 - n_c^2)]. \tag{4.3}$$

In the case when $\Delta n_c = 2N + 1$ the number n_v'' of intermediate states must coincide with the number n_c of initial states or the number n_c' of final states. Therefore the general

condition (4.2) takes the form

$$\begin{aligned} &\hbar\omega_0 = 2\gamma E_g && n_v'' = n_c' \\ &\omega_0\omega = (\pi V_z/d)^2(n_c'^2 - n_c^2) && n_v'' = n_c. \end{aligned} \tag{4.4}$$

One of the resonances (4.4) or both of them simultaneously can be observed in the spectral lines depending on ω_0. As one can see in figures 5 and 6 the spectral line $\Delta n_c = 1$ ($1.47 \times 10^{13}\ s^{-1} < \omega < 2.40 \times 10^{13}\ s^{-1}$) has two resonances at $\lambda_0 = 16.3\ \mu m$ (λ_0 is the wavelength of the incident radiation) and has one resonance at $\lambda_0 = 14.0\ \mu m$. The parameters of the energy spectrum of the electrons can be determined from the positions of the resonance peaks.

In conclusion we note that in a recent paper [13] the ERS process in size-quantized narrow-gap semiconductor films was investigated taking into account the mixing between the conduction and valence band states. The boundary condition in the form (2.10) was used. It was shown that the intraband ERS process with the intermediate state in the valence band is realized for $\Delta n_c = 2N + 1$ under certain conditions on the orientation of e_0 and e_1 with respect to the film surface.

Appendix

The wavefunctions (2.17) satisfy the condition

$$\hat{U}|\nu 1n\rangle = |\nu 2n\rangle \tag{A1}$$

where $\hat{U} = \hat{K}\hat{I}$ ($\hat{K}$ is the time inversion operator and $\hat{I}$ is the space inversion operator). Therefore only the coefficients for $|\nu 1n\rangle$ are given in the appendix:

$$\Gamma_{\nu\sigma n} = [1 + (\hbar\pi n/d)^2|\beta_{\nu\sigma n}|^2]^{-1/2}$$

$$G_{cn} = [(d/2)(K_0 + K_1 - E_g - 2E^c_{k_\perp n})(K_0 - E_g - E^c_{k_\perp n})]^{-1/2}$$

$$G_{vn} = [(d/2)(K_0 + K_1 - E_g - 2E^v_{k_\perp n})(K_1 - E^v_{k_\perp n})]^{-1/2}$$

$$\begin{aligned} A_{c1n} = &-(\beta_{c1n}\hbar k_x u_x - u_z)\varphi_1(r) - (\beta_{c1n}\hbar k_x t_x^* - t_z^*)\varphi_2(r) \\ &+ \beta_{c1n}(K_0 - E_g - E^c_{k_\perp n})\varphi_4(r) \end{aligned}$$

$$A_{v1n} = \beta_{v1n}(K_1 - E^v_{k_\perp n})\varphi_2(r) + (\beta_{v1n}\hbar k_x u_x - u_z)\varphi_3(r) - (\beta_{v1n}\hbar k_x t_x - t_z)\varphi_4(r)$$

$$\begin{aligned} B_{c1n} = &-[\hbar k_x u_x - (\hbar\pi n/d)^2\beta_{c1n}u_z]\varphi_1(r) - [\hbar k_x t_x^* \\ &- (\hbar\pi n/d)^2\beta_{c1n}t_z^*]\varphi_2(r) + (K_0 - E_g - E^c_{k_\perp n})\varphi_4(r) \end{aligned} \tag{A2}$$

$$\begin{aligned} B_{v1n} = &(K_1 - E^v_{k_\perp n})\varphi_2(r) + [\hbar k_x u_x - (n\hbar\pi/d)^2\beta_{v1n}u_z]\varphi_3(r) \\ &- [\hbar k_x t_x - (\hbar\pi n/d)^2\beta_{v1n}t_z]\varphi_4(r) \end{aligned}$$

$$\begin{aligned} \beta_{c1n} = &[u_z\varphi_1(\rho, z_0) + t_z^*\varphi_2(\rho, z_0)][\hbar k_x u_x\varphi_1(\rho, z_0) \\ &+ \hbar k_x t_x^*\varphi_2(\rho, z_0) - (K_0 - E_g - E^c_{k_\perp n})\varphi_4(\rho, z_0)]^{-1} \end{aligned}$$

$$\begin{aligned} \beta_{v1n} = &[u_z\varphi_3(\rho, z_0) - t_z\varphi_4(\rho, z_0)][(K_1 - E^v_{k_\perp n})\varphi_2(\rho, z_0) \\ &+ \hbar k_x u_x\varphi_3(\rho, z_0) - \hbar k_x t_x\varphi_4(\rho, z_0)]^{-1} \end{aligned}$$

$$E^{c,v}_{k_\perp n} = \tfrac{1}{2}(K_0 + K_1 - E_g) \pm [\tfrac{1}{4}(E_g + K_1 - K_c)^2 + (\hbar k_x V_x)^2 + (\hbar\pi n V_z/d)^2]^{1/2}.$$

We note that the Bloch amplitudes and the matrix elements of velocity are defined as

$$\begin{aligned}
&\varphi_1(r) = |\mathrm{v1}\rangle \qquad \varphi_2(r) = |\mathrm{v2}\rangle \qquad \varphi_3(r) = |\mathrm{c1}\rangle \qquad \varphi_4(r) = |\mathrm{c2}\rangle \\
&\hat{U}\varphi_1(r) = \varphi_2(r) \qquad \hat{U}\varphi_2(r) = -\varphi_1(r) \\
&\hat{U}\varphi_3(r) = -\varphi_4(r) \qquad \hat{U}\varphi_4(r) = \varphi_3(r) \\
&t = \langle \mathrm{v1}|v|\mathrm{c1}\rangle = \langle \mathrm{c2}|v|\mathrm{v2}\rangle \qquad u = \langle \mathrm{v1}|v|\mathrm{c2}\rangle = -\langle \mathrm{c1}|v|\mathrm{v2}\rangle \\
&\hat{U}t = -t^* \qquad \hat{U}t^* = -t \qquad \hat{U}u = -u^* \qquad \hat{U}u^* = -u \qquad \hat{U}r = -r \qquad \hat{U}p = p.
\end{aligned} \tag{A3}$$

As one can see from (A3), φ_1 and φ_2 (as well as φ_3 and φ_4) have different spins. At the same time $\varphi_1(\varphi_2)$ and $\varphi_3(\varphi_4)$ have contrary parities. If the film surface intersects the centre of the elementary cell, the Bloch amplitudes fixed on the surface have the following values: $\varphi_1(\varphi_2) = 0$ and $\varphi_3(\varphi_4) \neq 0$ (or vice versa). In the case when the film surface does not intersect the centre of elementary cell, all $\varphi_j(\boldsymbol{\rho}, z_0)$ have the same average value. On the other hand we can neglect the coordinate dependence of the Bloch amplitudes because the film thickness is much larger than the elementary cell sizes. In both cases the transformational properties of the Bloch amplitudes are taken into account in the calculation of the matrix elements of optical transitions.

References

[1] Genkin V N and Sokolov V V 1972 *Fiz. Tverd. Tela* **14** 1257
[2] Załuzny M 1983 *Thin Solid Films* **100** 169
[3] Riera R, Comas F, Trallero C Giner and Pavlov S T 1988 *Phys. Status Solidi* b **148** 533
[4] Ogrin Yu F, Lutskii V N and Elinson M I 1966 *Zh. Eksp. Teor. Fiz. Pis. Red.* **3** 114
[5] Abrikosov A A 1972 *J. Low Temp. Phys.* **8** 315
[6] Cohen M H 1961 *Phys. Rev.* **121** 387
[7] Luttinger J M and Kohn W 1955 *Phys. Rev.* **97** 869
[8] Volkov V A and Pinsker T N 1976 *Zh. Eksp. Teor. Fiz.* **70** 2268; 1977 *Zh. Eksp. Teor. Fiz.* **72** 1087
[9] Wallis R T and Mills D L 1970 *Phys. Rev.* B **2** 3312
[10] Gadzhiev A T, Gashimzade F M and Mustafaev N B 1988 *Fiz. Tverd. Tela* **30** 3146
[11] Belovolov M I, Brandt N B, Vavilov V S and Ponomarev Ya G 1977 *Zh. Eksp. Teor. Fiz.* **73** 721
[12] Mustafaev N B, Shakhtakhtinskii M G, Shteinshreiber V J and Gadzhiev A T 1986 *Thin Solid Films* **137** 7
[13] Okulski W and Zaluzny M 1989 *Phys. Status Solidi* b **155** 709